

## Application of H-Point Standard Addition Method and Multivariate Calibration Methods to the Simultaneous Kinetic-Potentiometric Determination of Permanganate and Dichromate

M.A. Karimi<sup>a,b,c,\*</sup>, R. Behjatmanesh-Ardakani<sup>a,c</sup>, M. Mazloum-Ardakani<sup>d</sup>, M.H. Mashhadizadeh<sup>e</sup> and F. Rahavian<sup>c</sup>  
<sup>a</sup>Payame Noor University, 19395-4697, Tehran, I.R. of Iran

<sup>b</sup>Department of Chemistry & Nanoscience and Nanotechnology Research Laboratory (NNRL), Faculty of Sciences, Payame Noor University, Sirjan, Iran

<sup>c</sup>Department of Chemistry, Faculty of Sciences, Payame Noor University, Ardakan, Iran

<sup>d</sup>Department of Chemistry, Faculty of Sciences, Yazd University, Yazd, Iran

<sup>e</sup>Department of Chemistry, Tarbiat Moallem University of Tehran, Tehran, Iran

(Received 4 December 2009, Accepted 1 October 2010)

Simultaneous kinetic-potentiometric determination of binary mixture of permanganate ( $\text{MnO}_4^-$ ) and dichromate ( $\text{Cr}_2\text{O}_7^{2-}$ ) by H-point standard addition method (HPSAM), partial least squares (PLS) and principal component regression (PCR) is described. In this work, the difference between the rate of the oxidation reaction of Fe(II) to Fe(III) in the presence of  $\text{MnO}_4^-$  and  $\text{Cr}_2\text{O}_7^{2-}$  formed the basis of the method. The rate of the consumed fluoride ion for making the complex was detected by a fluoride ion selective electrode (FISE). The results show that the simultaneous determination of  $\text{MnO}_4^-$  and  $\text{Cr}_2\text{O}_7^{2-}$  could be conducted in their concentration ranges of 0.5-10.0 and 0.1-20.0  $\mu\text{g ml}^{-1}$ , respectively. The total relative standard error (RSE) for applying the PLS and PCR methods to 9 synthetic samples was 5.30 and 3.17, respectively in the concentration range of  $\text{MnO}_4^-$ , and 3.30 and 2.04, respectively, in the concentration range of  $\text{Cr}_2\text{O}_7^{2-}$ . In order for the selectivity of the method to be assessed, we evaluated the effects of certain foreign ions upon the reaction rate. The proposed methods (HPSAM, PLS and PCR) were evaluated using a set of synthetic sample mixtures and then applied to the simultaneous determination of  $\text{MnO}_4^-$  and  $\text{Cr}_2\text{O}_7^{2-}$  in different water samples.

**Keywords:** Simultaneous determination, Permanganate, Dichromate, HPSAM, Multivariate calibration

---

### INTRODUCTION

Permanganate ( $\text{MnO}_4^-$ ) and dichromate ( $\text{Cr}_2\text{O}_7^{2-}$ ) are strong oxidants in chemistry that are used widely as oxidizing agents in diverse chemical reactions in the laboratory and industry for the synthesis of many different kinds of chemical compounds [1]. Permanganate is used as disinfectant, deodorizer, aquaculture, wastewater treatment, hydrogen sulfide

biomedicine and many others [2,3]. Dichromate is likewise a common inorganic chemical reagent, most commonly used as an oxidising agent in various laboratory and industrial applications [1]. It is also used to oxidise alcohols, determine ethanol, and clean laboratory glassware of organic contaminants [1,2]. In analytical chemistry, standardized aqueous solutions of  $\text{MnO}_4^-$  and  $\text{Cr}_2\text{O}_7^{2-}$  are sometimes used as oxidizing titrants for redox titrations. Therefore, determination of these oxidants is very important. Several methods have been reported for their determination such as

---

\*Corresponding author. E-mail: m\_karimi@pnu.ac.ir

spectrophotometry [4,5] and electroanalytical techniques [6]. Kinetic methods based on instrumental techniques in analytical chemistry are a developing subject, because of the growing need for analyzing the mixtures of trace species as well as similarities in the structure and behavior of these species [7]. On the other hand, by using modern computers and powerful software, kinetic methods in conjunction with chemometrics make it possible to analyze multicomponent mixtures without separation. Through this approach, it is possible to attain greater selectivity with high speed of analysis and very low detection limit using cheap methods such as potentiometry. In the area of simultaneous determination of  $\text{MnO}_4^-$  and  $\text{Cr}_2\text{O}_7^{2-}$  mixture, in which both are strong oxidants and have color, there is only one report in literature based on the difference in the oxidation rate of pyrogallol red (PGR) by spectrophotometry [8]. There is another report on the mixture of vanadate and permanganate [9] which is based on the difference observed in the reaction rate of oxidation of PGR with binary mixture of permanganate and vanadate. However, to the best of our knowledge, there is no report regarding the simultaneous determination of  $\text{MnO}_4^-$  and  $\text{Cr}_2\text{O}_7^{2-}$  by electroanalytical techniques using HPSAM and chemometric methods.

In recent years, the adoption of chemometric methods in electroanalytical chemistry, as in other areas of analytical chemistry, has received considerable attention as these methods are helpful in the extraction of adequate information from the experimental data. Electroanalytical techniques are well known as the excellent and cheap procedures for the determination of trace chemical species. Applications of H-point standard addition method (HPSAM) and chemometric techniques including artificial neural network (ANN), partial least squares (PLS) and principal component regression (PCR) have been frequently reported for the calibration of overlapping voltammetric signals [10-15]. In the field of potentiometry, several methods have been reported based on flow injection system and titration using PLS, ANN and Kalman filter as the modeling methods [16-22]. Herin, we report the first application of PLS and PCR multivariate calibration methods and HPSAM to the simultaneous kinetic-potentiometric determination of binary mixtures of hydrazine and its derivatives [23,24] and binary mixture of levodopa and carbidopa drugs [25]. The methods are based on the

differences observed in the production rate of chloride ions in the reaction of these species with *N*-chlorosuccinimide. The reaction rate of the production of chloride ion was monitored by a chloride ion-selective electrode. Recently, we also reported the applications of HPSAM, PLS and PCR for the simultaneous determination of binary and ternary mixtures of Fe(III), Al(III) and Zr(IV) [26,27]. These methods were based on the complex forming reaction of these metallic ions with fluoride ion that has a differential rate at certain reaction conditions. Therefore, the rate of fluoride-ion reaction with Fe(III), Al(III) and Zr(IV) was monitored by a fluoride ion-selective electrode (FISE).

This work reports the first application of HPSAM, PCR and PLS as chemometric methods to the simultaneous determination of  $\text{MnO}_4^-$  and  $\text{Cr}_2\text{O}_7^{2-}$  using potentiometric technique. The methods are based on the difference observed in the oxidation reaction rate of Fe(II) and Fe(III) in the presence of  $\text{MnO}_4^-$  and  $\text{Cr}_2\text{O}_7^{2-}$  as oxidants and complexing reaction between Fe(III) and fluoride ion at certain reaction conditions. The very fast response of the FISE and its Nernstian behavior with respect to fluoride ions in acidic solutions indicated that this electrode might be employed effectively in the kinetic studies of reactions involving changes in the fluoride ion concentration [22]. Therefore, the rate of the complexing reaction of the fluoride ion with Fe(III) was monitored by an FISE.

## EXPERIMENTAL

### Apparatus and Software

A solid-state Fluoride-selective electrode (Metrohm Model 6.0502.150) was used in conjunction with a double junction Ag/AgCl reference electrode (Metrohm Model 6.0726.100), whose outer compartment was filled with a saturated KCl solution. The Metrohm Model 780 potentiometer, attached to a Pentium(IV) computer, was used for recording the kinetic potentiometric data. All measurements were carried out in a thermostated ( $25.0 \pm 0.2$  °C), double-walled reaction cell with continuous magnetic stirring. The electrode was stored in  $1 \times 10^{-3}$  M potassium fluoride solution when not in use. For pH measurements, a Metrohm Model 780 pH meter with combination glass electrode was used. Chemometric analysis

was performed using MATLAB 7.0 program.

### Materials and Reagents

All chemicals were of analytical reagent grade and doubly distilled water was used throughout. A stock solution of iron (1000  $\mu\text{g ml}^{-1}$ ) was prepared by dissolving 0.524 g of iron(II) sulfate ( $\text{FeSO}_4 \cdot 7\text{H}_2\text{O}$ ) in water and then diluting it to 100 ml. Stock solutions  $\text{MnO}_4^-$  and  $\text{Cr}_2\text{O}_7^{2-}$  were prepared in 100-ml flasks by dissolving 0.1329 g of potassium permanganate and 0.1369 g of potassium dichromate in water and diluting with water to the mark. Permanganate concentration was determined by redox titration with potassium oxalate. Potassium permanganate and potassium dichromate and salts of Fe(II) and fluoride were purchased from Merck (Germany). Citrate buffer solution (0.1 M, pH 3.0) was prepared using solutions of 0.1 M citric acid, 0.1 M  $\text{HNO}_3$  and 0.1 M NaOH adjusting its pH with a pH meter.

### Procedure

Twenty five milliliters of double-distilled water, 2.0 ml of buffer solution, 1.0 ml of standard fluoride solution (0.1 M) and 1.0 ml of  $5 \times 10^{-3}$  M of iron(II) solution were added to the thermostated ( $25.0 \pm 0.2$  °C) reaction cell. Five milliliter of the standard or sample solution of  $\text{Cr}_2\text{O}_7^{2-}$ ,  $\text{MnO}_4^-$ , or a mixture of them, were injected into the cell quickly, and after the stabilization of the potential (about 30 s), all data were recorded. The potential changes versus time were recorded at the time intervals of 1.0 s. Synthetic samples containing different concentration ratios of  $\text{Cr}_2\text{O}_7^{2-}$  and  $\text{MnO}_4^-$  were prepared and standard additions of  $\text{Cr}_2\text{O}_7^{2-}$  were made. The simultaneous determination of  $\text{Cr}_2\text{O}_7^{2-}$  and  $\text{MnO}_4^-$  was conducted by recording the potential changes for each solution from 30 to 500 s. After each run the cell was emptied and washed twice with doubly distilled water.

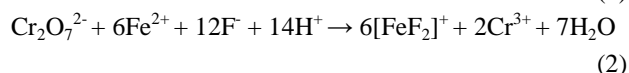
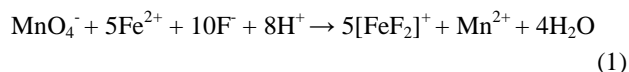
Using the standard analyte solutions, we can construct a calibration graph of ( $10^{\Delta E/S} - 1$ ) vs. concentration (fixed-time method) [28], where  $\Delta E$  is the potential variation in a selected time interval  $\Delta t$  and  $S$  is the slope of the fluoride electrode response, which is determined periodically by successive additions of micro-amounts of 100  $\mu\text{l}$  of  $1.0 \times 10^{-4}$ - $1.0 \times 10^{-1}$  M of NaF standard solutions in 25.0 ml of water mixed with 2.0 ml of buffer solution.

The simultaneous determination of  $\text{Cr}_2\text{O}_7^{2-}$  and  $\text{MnO}_4^-$

standard solutions with HPSAM was performed by measuring the potential changes ( $\Delta E$ ) at 200 and 300 s after initiation of the reaction for each sample solution. Then plots of HPSAM of ( $10^{\Delta E/S} - 1$ ) vs. the added concentration of  $\text{Cr}_2\text{O}_7^{2-}$  were constructed for the mixtures of  $\text{Cr}_2\text{O}_7^{2-}$  and  $\text{MnO}_4^-$ . The simultaneous determination of  $\text{Cr}_2\text{O}_7^{2-}$  and  $\text{MnO}_4^-$  adopting PLS and PCR methods was performed by recording the potential for each solution from 30 to 500 s.

## RESULTS AND DISCUSSION

We need to find a system that shows different kinetic behavior for the reaction with  $\text{Cr}_2\text{O}_7^{2-}$  and  $\text{MnO}_4^-$ . It is well-known that the rate of oxidation of  $\text{Fe}^{2+}$  with  $\text{MnO}_4^-$  is much higher than that with  $\text{Cr}_2\text{O}_7^{2-}$  [8,29]. Therefore, we could use this different kinetic behavior for the simultaneous determination of  $\text{Cr}_2\text{O}_7^{2-}$  and  $\text{MnO}_4^-$ . The concept of the simultaneous analysis of  $\text{Cr}_2\text{O}_7^{2-}$  and  $\text{MnO}_4^-$  in this work is based on the difference in their oxidizing power. Preliminary studies showed that iron(II) ion as reagent in the presence of fluoride ion using FISE was suitable for our purpose. Upon the addition of the oxidant ( $\text{MnO}_4^-$  and/or  $\text{Cr}_2\text{O}_7^{2-}$ ) into the solution of  $\text{Fe}^{2+}$  in the presence of  $\text{F}^-$ , the oxidation reaction of  $\text{Fe}^{2+}$  with  $\text{MnO}_4^-$  and  $\text{Cr}_2\text{O}_7^{2-}$  takes place as follows:



In order to initiate the simultaneous kinetic potentiometric determination of  $\text{Cr}_2\text{O}_7^{2-}$  and  $\text{MnO}_4^-$  by HPSAM, PCR and PLS, a series of experiments was conducted to establish the optimum system to achieve maximum sensitivity. Therefore, all experimental parameters affecting the reaction rate of  $\text{Fe}^{2+}$  with  $\text{MnO}_4^-$  and  $\text{Cr}_2\text{O}_7^{2-}$  (response time, concentration of  $\text{F}^-$  and  $\text{Fe}^{2+}$ , pH, etc.) were carefully optimized.

### Study of the Electrode Characteristics

The remarkably fast response of FISE and its Nernstian behavior toward fluoride ions in acidic solutions indicates that this electrode might be employed effectively in the kinetic studies of reactions involving changes in the fluoride ion concentration [21]. The characteristics of the fluoride-selective

electrode in the HNO<sub>3</sub>- citric acid -NaOH buffer were studied. In order to evaluate the operating characteristics of the FISE at pH < 5, calibration graphs were constructed for sodium fluoride in the concentration range of  $2.0 \times 10^{-6}$ - $1.0 \times 10^{-2}$  M at pHs 4.0, 3.0, 2.5 and 2.0. The slope was found to be 56.8 mV decade<sup>-1</sup> and remained almost constant at 0.2 mV over 7 months of use in this system at pH 2.5.

### Effect of Fluoride and Iron(II) Concentrations

The effect of F<sup>-</sup> concentration over the ranges of  $1.0 \times 10^{-5}$ - $1.0 \times 10^{-2}$  M fluoride ion on the linear range of calibration graph and reaction rate with Fe(II) was investigated. When the concentration of F<sup>-</sup> was low, a gradual slope in the calibration graph was realized while a high concentration of F<sup>-</sup> generated a high steep slope in the calibration graph. The results also indicated that the concentration of F<sup>-</sup> had a significant effect on the linear range and on the change in the potential value. So, the fluoride concentration must have been excessive. However, by increasing the fluoride concentration, the potential change was decreased and the sensitivity was lower. If the fluoride concentration had been too low, the potential not have been steady. Since maximum difference in the kinetic behavior of Fe(III) (resulting from oxidation reaction of Fe<sup>2+</sup> to Fe<sup>3+</sup> by MnO<sub>4</sub><sup>-</sup> and Cr<sub>2</sub>O<sub>7</sub><sup>2-</sup>) was observed in a concentration of  $1.0 \times 10^{-3}$  M fluoride, and since both species had larger values of potential change ( $\Delta E$ ) in this concentration, it was selected as the optimum concentration for further studies.

The effect of Fe<sup>2+</sup> concentration over the ranges of  $1.0 \times 10^{-5}$ - $1.0 \times 10^{-1}$  M Fe<sup>2+</sup> ion on the reaction rate of Fe<sup>2+</sup> with MnO<sub>4</sub><sup>-</sup> and Cr<sub>2</sub>O<sub>7</sub><sup>2-</sup> as well as the linear range of calibration graph were investigated. The results show that the increase of Fe<sup>2+</sup> concentration, up to  $5.0 \times 10^{-3}$  M, causes an increase in the reaction rate of Fe<sup>2+</sup> with both MnO<sub>4</sub><sup>-</sup> and Cr<sub>2</sub>O<sub>7</sub><sup>2-</sup> and the potential change, but causes a decrease at higher concentrations. Therefore, a concentration of  $5.0 \times 10^{-3}$  M Fe<sup>2+</sup> ion was selected as the optimum concentration for further studies.

### Effect of pH

Acidity of the solution influences the potential response of FISE, the oxidation reaction rate of Fe<sup>2+</sup> with MnO<sub>4</sub><sup>-</sup> and Cr<sub>2</sub>O<sub>7</sub><sup>2-</sup> and the complexity of the reaction rate of F<sup>-</sup> with Fe<sup>3+</sup>. Direct measurement of the free fluoride concentration in acidic

solution, could be fully explained in terms of the species F<sup>-</sup>, HF, HF<sub>2</sub><sup>-</sup> and (HF)<sub>2</sub> if they are assumed to be ideal Nernstian responses of the electrode [30].

The cell potential is given in Eq. (3) as follows:

$$E = E' + S \log[F^-] \quad (3)$$

where  $E$ ,  $E'$ ,  $S$  and  $F^-$  are the potential, formal potential, slope of the fluoride electrode response and the free fluoride concentration, respectively. At a constant pH in acidic solution, the free and total fluoride (TF) concentrations are in a fixed ratio to one another in the concentration range of  $2.0 \times 10^{-6}$ - $1.0 \times 10^{-2}$  M [31], so that

$$E = E' + S \log[TF] \quad (4)$$

The reaction of Fe<sup>3+</sup> with F<sup>-</sup> occurs in acidic solution (at pH ≤ 2) whose reaction rate depends on the concentration of the free F<sup>-</sup> and the concentration of the free F<sup>-</sup> depends on pH, therefore, the rate of the formation of FeF<sup>2+</sup> is pH dependent [31].

When the pH was altered from 2.0 to 5.0, a moderate decrease in the average rate was recorded (the total potential change was about 5 mV less), apparently owing to the hydrolyzed species of Fe<sup>3+</sup> (FeOH<sup>2+</sup>, Fe(OH)<sub>2</sub><sup>+</sup>), providing additional paths with a rate proportional to [F<sup>-</sup>].

The results show that the maximum difference in kinetic behavior of Fe<sup>3+</sup> was observed at pH 3.0. In addition, Fe<sup>3+</sup> had larger values of potential change ( $\Delta E$ ) at this pH. Above pH 3.0, the potential change decreased evidently due to the occurrence of the hydrolysis reaction competing with the complexity of the reaction between the fluoride and Fe<sup>3+</sup>. Under pH 3.0, the potential change decreased, too, probably owing to the formation of hydrogen fluoride, to which the fluoride electrode is insensitive. Thus, pH 3.0 was selected as the optimum pH for further studies.

### Composition Effect of Ground Buffer Solution

The change of potential value ( $\Delta E$ ) for the reaction of Fe<sup>2+</sup> with MnO<sub>4</sub><sup>-</sup> and Cr<sub>2</sub>O<sub>7</sub><sup>2-</sup> in the presence of certain amount of the fluoride ion in different acidic solutions is shown in Table 1. In the solution of HNO<sub>3</sub>- citric acid -NaOH (pH 3.0),  $\Delta E_{Fe^{3+}}$  had larger values. According to the obtained results,

**Table 1.** The Values of  $\Delta E$  for Reaction of  $10 \mu\text{g ml}^{-1}$  of  $\text{Fe}^{2+}$  with  $\text{MnO}_4^-$  and  $\text{Cr}_2\text{O}_7^{2-}$  in the Presence of  $1.0 \times 10^{-3}$  M  $\text{F}^-$  Ion in Different Acid Solutions (pH = 3.0)

Acid solution	$\text{HNO}_3$ - $\text{H}_3\text{PO}_4$ -NaOH	KCl-HCl	$\text{HNO}_3$ -Tartaric acid-NaOH	$\text{HNO}_3$ -Citric acid- NaOH
$\Delta E_{\text{Fe}^{3+}}$ (mV)	2.3	7.5	8.5	13

the 0.1 M citric acid-0.1 M nitric acid-0.1 M sodium hydroxide mixed solution (pH 3.0) containing  $1.0 \times 10^{-3}$  M fluoride was chosen as the ground buffer solution.

### Temperature Effect

The temperature of the solution evidently affects the reaction rate of the kinetic reaction. But higher temperatures do not have any positive effect on the difference between the rate of the oxidation of Fe(II) to Fe(III) in the presence of  $\text{MnO}_4^-$  and  $\text{Cr}_2\text{O}_7^{2-}$  and the complexing reaction of  $\text{Fe}^{3+}$  with fluoride. Therefore, the temperature of the solution was kept at  $25 \pm 0.2$  °C by a thermostatic water bath in all of the measurements.

### Potential-Time Behavior

The potential-time behavior of the reactions of  $\text{Fe}^{2+}$  with  $\text{MnO}_4^-$  and  $\text{Cr}_2\text{O}_7^{2-}$  in the presence of  $\text{F}^-$  under the optimized conditions is shown in Fig. 1. Figure 2 shows typical reaction curves for the reaction of  $\text{Fe}^{2+}$  with  $\text{MnO}_4^-$  and  $\text{Cr}_2\text{O}_7^{2-}$  at different concentrations. As can be seen in Figs. 1 and 2, the reaction of  $\text{MnO}_4^-$  was faster than  $\text{Cr}_2\text{O}_7^{2-}$  and was almost completed in 100 s after the initial reaction but the reaction of  $\text{Cr}_2\text{O}_7^{2-}$  was completed in almost 300 s. This difference in the reaction rates allowed us to design the HPSAM, PCR and PLS methods for the simultaneous determination of  $\text{MnO}_4^-$  and  $\text{Cr}_2\text{O}_7^{2-}$ .

Characteristics of calibration graphs for the determination of  $\text{MnO}_4^-$  and  $\text{Cr}_2\text{O}_7^{2-}$ , under the optimum conditions, are given in Table 2.

### Requirements for Applying HPSAM

The concept of using HPSAM to treat the kinetic data upon the completion of the reaction of one component while of the reaction of the other component is not yet completed, is described below. The variables to be fixed were time variables

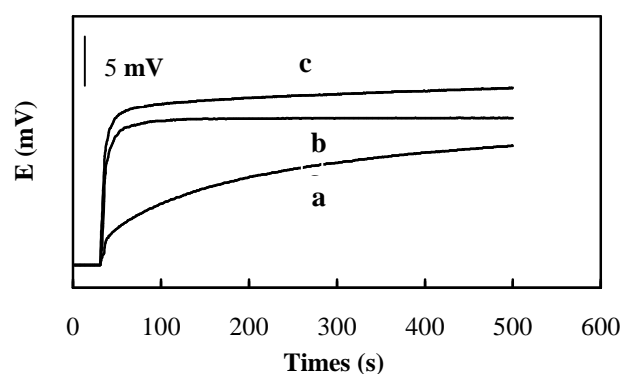


**Fig. 1.** Potential-time curves for the reaction of  $\text{F}^-$  and  $\text{Fe}^{2+}$  with  $10 \mu\text{g ml}^{-1}$  of  $\text{Cr}_2\text{O}_7^{2-}$ , (a),  $5 \mu\text{g ml}^{-1}$  of  $\text{MnO}_4^-$  (b) and mixture of them (c). Other conditions were constant as follows:  $1.0 \times 10^{-3}$  M  $\text{F}^-$ ;  $5.0 \times 10^{-3}$  M  $\text{Fe}^{2+}$ ; 0.1 M citric acid-0.1 M  $\text{HNO}_3$ -0.1 M NaOH mixed solution (pH 3.0);  $T = 25 \pm 0.2$  °C.

$t_1$  and  $t_2$  and the product of the reaction of  $\text{Cr}_2\text{O}_7^{2-}$  had the same amount of  $R$  (or  $10^{\Delta E/S} - 1$ ) over the interval between these two times. Moreover, there was an appropriate difference between the slopes of the calibration lines in this interval.

Considering a binary mixture of  $\text{MnO}_4^-$  and  $\text{Cr}_2\text{O}_7^{2-}$ , for example, assume that the amount of  $(10^{\Delta E/S} - 1)$  of the oxidation in the reaction of  $\text{Fe}^{2+}$  with  $\text{Cr}_2\text{O}_7^{2-}$  and then complexation in the reaction of  $\text{Fe}^{3+}$  with  $\text{F}^-$  at time variables  $t_1$  and  $t_2$  were  $P_i$  and  $Q_i$ , respectively, while those for the  $\text{MnO}_4^-$ - $\text{Fe}^{2+}$ - $\text{F}^-$  reaction under the same conditions were  $P$  and  $Q$ , respectively (Fig. 3). They were equal in this case. The following equations show the relation between them:

$$\text{For } \text{Cr}_2\text{O}_7^{2-}: Q_i = P_i + m_i t_j \quad (t_1 \leq t_j \leq t_2; i = 0, 1, \dots, n) \quad (5)$$

$$\text{For } \text{MnO}_4^-: Q = P + m t_j \quad (m = 0) \quad (6)$$

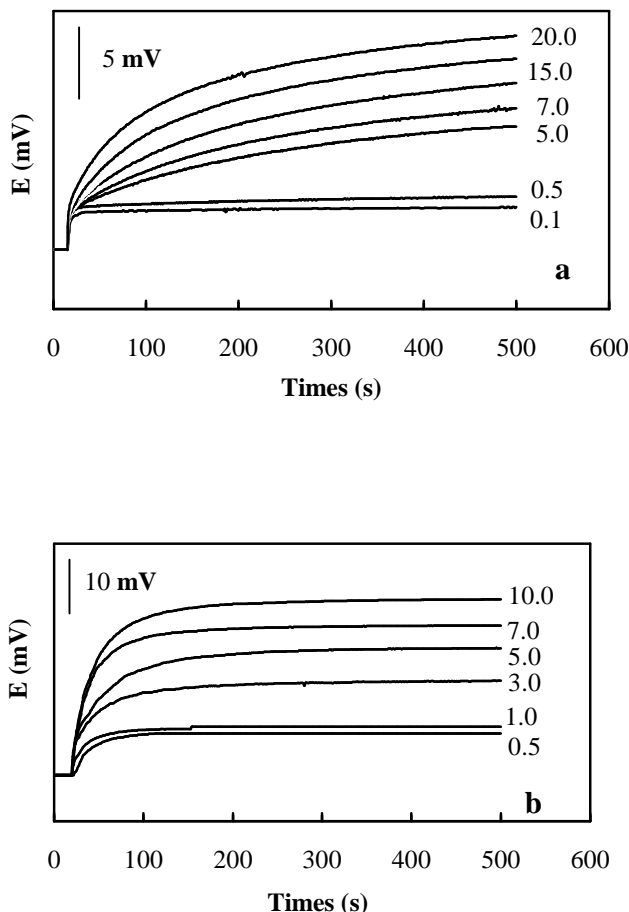


**Fig. 2.** Typical potential-time curves for the reaction of  $F^-$  and  $Fe^{2+}$  with  $MnO_4^-$  (a) and  $Cr_2O_7^{2-}$  (b) at different concentrations ( $\mu g\ ml^{-1}$ ). Other conditions were constant as in Fig. 1.

where the subscripts  $i$  and  $j$  denote different solutions for  $n$  additions of  $Cr_2O_7^{2-}$  concentration prepared to apply to HPSAM and the time comprising the  $t_1$ - $t_2$  range, respectively. Thus, the overall amounts of  $(10^{\Delta E/S}-1)$  (or  $R$ ) of the  $MnO_4^-$ - $Cr_2O_7^{2-}$  mixture are:

$$\text{At } t_1 \quad R_{t_1} = P + P_i \quad (7)$$

$$\text{At } t_2 \quad R_{t_2} = Q + Q_i \quad (8)$$

The simultaneous kinetic determination of the concentration of  $MnO_4^-$  and  $Cr_2O_7^{2-}$  by HPSAM requires the selection of two times  $t_1$  and  $t_2$ . To select the appropriate times, the following principles were observed. At the two selected times  $t_1$  and  $t_2$ , the amount of  $R$  of the  $Cr_2O_7^{2-}$  must be linear with the concentrations, and the amount of  $R$  for  $Fe^{3+}$  must remain constant even if the  $MnO_4^-$  concentrations are changed. The amount of  $R$  for the mixture of  $MnO_4^-$  and  $Cr_2O_7^{2-}$  should be equal to the sum of the individual  $R$ s of the two compounds. In addition, the slope difference of the two straight lines obtained at both  $t_1$  and  $t_2$  must be as large as possible to achieve good accuracy. Then known amounts of  $Cr_2O_7^{2-}$  have to be successively added to the mixture and the resulting potential changes to be measured at the two times as expressed below.

$$R_{t_1} = (10^{\Delta E(t_1)/S}-1)_{t_1} = P_0 + P + M_{t_1}C_i \quad (9)$$

$$R_{t_2} = (10^{\Delta E(t_2)/S}-1)_{t_2} = Q_0 + Q + M_{t_2}C_i \quad (10)$$

where  $\Delta E(t_1)$  and  $\Delta E(t_2)$  are the potential changes measured at

**Table 2.** Characteristics of Calibration Graphs for the Determination of  $MnO_4^-$  and  $Cr_2O_7^{2-}$

Species	Linear range ( $\mu g\ ml^{-1}$ )	Slope ( $ml\ \mu g^{-1}$ )	Intercept	Correlation coefficient	LOD & LOQ ( $\mu g\ ml^{-1}$ ) <sup>a</sup>
$MnO_4^-$	0.5-10.0	0.3008	0.2635	0.9992 (n = 7)	0.028 & 0.070
$Cr_2O_7^{2-}$	0.1-20.0	0.1118	0.3095	0.9995 (n = 11)	0.086 & 0.226

<sup>a</sup>Limit of detection (LOD) and limit of quantitation (LOQ) are the mean blank value plus three and ten times the standard deviation of the blank, respectively.

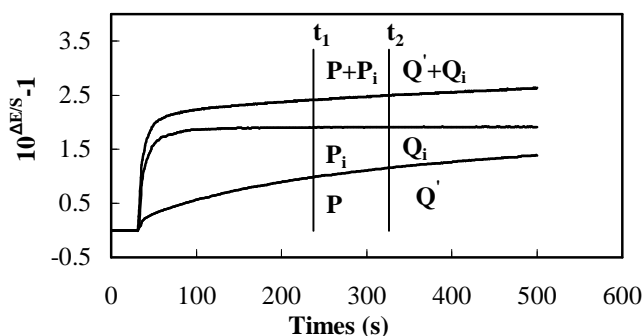


**Fig. 3.** Plot of potential changes ( $10^{\text{AE/S}}-1$ ) for the reaction of  $\text{F}^-$  and  $\text{Fe}^{2+}$  with  $5 \mu\text{g ml}^{-1}$   $\text{Cr}_2\text{O}_7^{2-}$  (a),  $10 \mu\text{g ml}^{-1}$   $\text{MnO}_4^-$  (b) and mixture of them (c). Other conditions were constant as in Fig. 1.

$t_1$  and  $t_2$ , respectively and  $S$  is the slope of the fluoride electrode response.  $P_0$  and  $Q_0$  are the amounts of  $R$  for  $\text{Cr}_2\text{O}_7^{2-}$  at a sample at  $t_1$  and  $t_2$ , respectively.  $P$  and  $Q$  are the amounts of  $R$  for  $\text{MnO}_4^-$  at  $t_1$  and  $t_2$ , respectively (Fig. 4).  $M_{t1}$  and  $M_{t2}$  are the slopes of the standard addition calibration lines at  $t_1$  and  $t_2$ , respectively.  $C_i$  is the added  $\text{Cr}_2\text{O}_7^{2-}$  concentration. The two obtained straight lines intersect at the so-called H-point ( $-C_H, R_H$ ) (Fig. 4). Since  $R_{t1} = R_{t2}$ ,  $H(-C_H, R_H) \approx (-C_{\text{Dichromate}}, R_{\text{Permanganate}})$  from Eqs. (5) and (6) we have:

$$P_0 + P + M_{t1}(-C_H) = Q_0 + Q + M_{t2}(-C_H) \quad (11)$$

$$-C_H = [(Q - P) + (Q_0 - P_0)] / (M_{t1} - M_{t2}) \quad (12)$$

as species  $\text{MnO}_4^-$  is assumed not to evolve over the considered range of time,

$$Q = P$$

and

$$C_H = (Q_0 - P_0) / (M_{t1} - M_{t2}) \quad (13)$$

which is equivalent to the existing  $C_{\text{Dichromate}} (=P_0/M_{t1} = Q_0/M_{t2})$ . Combining this with Eq. (9) yields  $R_H = P$ . The overall equation for the potential at the H-point is simply represented as:

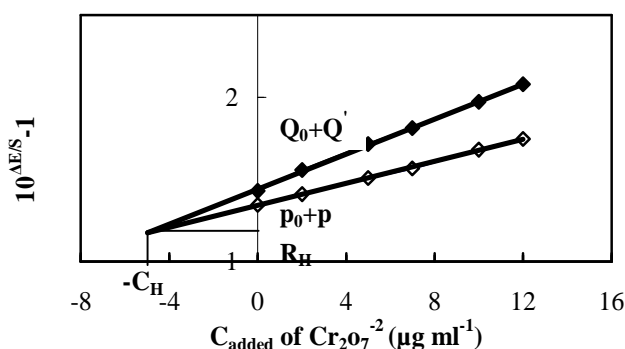


**Fig. 4.** Plot of HPSAM for simultaneous determination of a mixture of  $\text{Cr}_2\text{O}_7^{2-}$  ( $5.0 \mu\text{g ml}^{-1}$ ) and  $\text{MnO}_4^-$  ( $3.0 \mu\text{g ml}^{-1}$ ). Other conditions were constant as in Fig. 1.

$$Q = P = R_H = R_{Fe} \quad (14)$$

The intersection of the straight lines in Eqs. (9) and (10) directly yields the unknown  $\text{Cr}_2\text{O}_7^{2-}$  concentration ( $C_{\text{Dichromate}}$ ) and the  $R$  for  $\text{MnO}_4^-$  species ( $R_{\text{Permanganate}}$ ) corresponding to  $t_1$  and  $t_2$  in the original samples, as the two times were chosen in such a way that the later species had the same  $R$  at both times. This analytical signal allows the calculation of the concentration of  $\text{MnO}_4^-$  from a calibration curve.

Since  $\text{Cr}_2\text{O}_7^{2-}$  was selected as the analyte, it was possible to select several pairs of time ranges which presented the same  $R$  for  $\text{MnO}_4^-$ . Some of the selected time pairs were 100-200, 100-250, 100-300, 200-300 and 200-400 s. Greater time increments caused higher sensitivity and steeper slopes of the two time axes, as shown previously by Campins-Falco *et al.* [32]. Also, the accuracy of the determinations was affected by the slope increments of H-point plots. However, the time pair that gave the greatest slope increment, lower error, and the shortest analysis time was selected. For this reason, the time pair of 100-300 s as the most suitable times was employed.

A summary of the results obtained for various analyte concentrations is given in Tables 3 and 4. The concentration was calculated directly by solving a system of equations of two straight lines.  $\text{MnO}_4^-$  concentrations were calculated in each test solution by the calibration method with a single standard and ordinate value of  $R$ .

**Table 3.** Results of Several Experiments for Analysis of  $\text{MnO}_4^-$  and  $\text{Cr}_2\text{O}_7^{2-}$  Mixtures in Different Concentration Ratios Using HPSAM (T = 25 °C)

R-C equation	r	Spiked ( $\mu\text{g ml}^{-1}$ )		Found ( $\mu\text{g ml}^{-1}$ )	
		$\text{MnO}_4^-$	$\text{Cr}_2\text{O}_7^{2-}$	$\text{MnO}_4^-$	$\text{Cr}_2\text{O}_7^{2-}$
$R_{300} = 0.4120C_i + 1.3806$	0.9998	5.0	5.0	$4.85 \pm (0.11)^a$	$5.15 \pm (0.11)^a$
$R_{100} = 0.2420C_i + 1.3347$	0.9999				
$R_{300} = 0.2140C_i + 2.1178$	0.9995	8.0	6.0	$8.24 \pm (0.18)^a$	$6.10 \pm (0.14)^a$
$R_{100} = 0.1390C_i + 2.0528$	0.9980				
$R_{300} = 0.3261C_i + 1.9715$	0.9903	5.0	4.0	$5.16 \pm (0.11)^a$	$4.19 \pm (0.08)^a$
$R_{100} = 0.2559C_i + 1.6767$	0.9962				
$R_{300} = 0.3723C_i + 1.9080$	0.9968	1.0	12.0	$1.20 \pm (0.10)^a$	$12.23 \pm (0.21)^a$
$R_{100} = 0.0640C_i + 0.3433$	0.9908				
$R_{300} = 0.3590C_i + 0.7793$	0.9997	5.0	1.0	$4.80 \pm (0.08)^a$	$1.02 \pm (0.05)^a$
$R_{100} = 0.2890C_i + 0.7002$	0.9990				
$R_{300} = 0.2018C_i + 1.6302$	0.9972	10.0	3.0	$9.95 \pm (0.16)^a$	$3.08 \pm (0.04)^a$
$R_{100} = 0.1549C_i + 1.4855$	0.9981				
$R_{300} = 0.2765C_i + 3.2547$	0.9984	8.0	7.0	$8.20 \pm (0.23)^a$	$7.24 \pm (0.12)^a$
$R_{100} = 0.1813C_i + 2.4886$	0.9907				
$R_{300} = 0.2329C_i + 1.0079$	0.9966	2.0	0.5	$2.02 \pm (0.03)^a$	$0.52 \pm (0.10)^a$
$R_{100} = 0.0743C_i + 0.5181$	0.9969				

<sup>a</sup>Standard deviation (s) is in parenthesis and the results are averages of three replicates.

**Table 4.** Results of Five Replicate Experiments for Analysis of  $\text{Cr}_2\text{O}_7^{2-}$  and  $\text{MnO}_4^-$  Mixture Using HPSAM (T = 25 °C)

R-C equation	r	Spiked ( $\mu\text{g ml}^{-1}$ )		Found ( $\mu\text{g ml}^{-1}$ )	
		$\text{Cr}_2\text{O}_7^{2-}$	$\text{MnO}_4^-$	$\text{Cr}_2\text{O}_7^{2-}$	$\text{MnO}_4^-$
$R_{300} = 0.3460C_i + 1.4986$	0.9999	5.0	3.0	4.82	3.10
$R_{100} = 0.1910C_i + 1.4246$	0.9986				
$R_{300} = 0.5330C_i + 1.4411$	0.9995	5.0	3.0	5.20	3.03
$R_{100} = 0.3350C_i + 1.3428$	0.9995				
$R_{300} = 0.2610C_i + 1.2098$	0.9986	5.0	3.0	4.90	2.90
$R_{100} = 0.0860C_i + 1.1246$	0.9999				
$R_{300} = 0.2020C_i + 1.1845$	0.9994	5.0	3.0	5.20	2.80
$R_{100} = 0.0420C_i + 1.1012$	0.9950				
$R_{300} = 0.1900C_i + 1.1809$	0.9993	5.0	3.0	4.80	2.90
$R_{100} = 0.0670C_i + 1.1147$	0.9960				
Mean				4.92	2.95
RSD (%)				2.03	3.39

### Multivariate Calibration

The applications of chemometric methods such as PCR and PLS, to the analysis of multi-component mixtures, have been discussed by several workers [33-37]. PCR and PLS modelings are powerful multivariate statistical tools, which are successfully applied to the quantitative analysis of spectrochemical and electrochemical data [23-27,33-39]. The first step in the simultaneous determination of the species by PCR and PLS methodologies involves the construction of a calibration matrix for the binary mixture of  $\text{MnO}_4^-$  and  $\text{Cr}_2\text{O}_7^{2-}$ . For constructing the calibration set, factorial design was applied to five levels in order to extract detailed quantitative information, using only a few experimental trials. In this research, a synthetic set of 37 solutions, including different concentrations of  $\text{MnO}_4^-$  and  $\text{Cr}_2\text{O}_7^{2-}$ , was prepared. A collection of 28 solutions was selected as the calibration set (Table 5) and the other 9 solutions were used as the prediction set (Table 6). Their composition was randomly designed to obtain more information from the calibration procedure. Changes in the solution potential were recorded during a time period of 300 s.

To select the number of factors in the PCR and PLS

algorithm, as a cross-validation method, leaving out one sample method was employed [40]. The prediction error was calculated for each species of the prediction set. This error was expressed as the prediction residual error sum of squares (PRESS):

$$PRESS = \sum_{i=1}^m \left( \hat{C}_i - C_i \right)^2 \quad (15)$$

where  $m$  is the total number of calibration sample,  $\hat{C}_i$  represents the estimated concentration while  $C_i$  is the reference concentration for the  $i$ th sample left out of the calibration during the cross validation. Figure 5 shows a plot of PRESS against the number of factors for a mixture of components. To find out the minimum factors, we also used the F-statistics to carry out the significant determination [41]. The optimal number of factors, for the two components, was obtained as 2 for both PCR and PLS.

For evaluating the predictive ability of a multivariate calibration model, the root mean square error of prediction (RMSEP), relative standard error of prediction (RSEP) and

**Table 5.** Calibration Set for Constructing PCR and PLS Methods in Determination of  $\text{MnO}_4^-$  and  $\text{Cr}_2\text{O}_7^{2-}$  ( $\mu\text{g ml}^{-1}$ )

Sample number	$\text{MnO}_4^-$	$\text{Cr}_2\text{O}_7^{2-}$	Sample number	$\text{MnO}_4^-$	$\text{Cr}_2\text{O}_7^{2-}$
1	0.5	0.5	15	5.0	5.0
2	0.5	1.0	16	5.0	10.0
3	0.5	5.0	17	5.0	12.0
4	0.5	7.0	18	5.0	15.0
5	0.5	19.0	19	7.0	19.0
6	2.0	4.0	20	7.0	12.0
7	2.0	10.0	21	7.0	15.0
8	2.0	16.0	22	7.0	17.0
9	2.0	18.0	23	7.0	2.0
10	2.0	20.0	24	10.0	4.0
11	4.0	6.0	25	10.0	8.0
12	4.0	10.0	26	10.0	10.0
13	4.0	14.0	27	10.0	12.0
14	4.0	16.0	28	10.0	16.0

**Table 6.** Prediction Set for Constructing PLS and PCR Models in Determination of  $\text{Cr}_2\text{O}_7^{2-}$  and  $\text{MnO}_4^-$  and Statistical Parameters Calculated for these Models

Solution	Synthetic ( $\mu\text{g ml}^{-1}$ )		Predicted ( $\mu\text{g ml}^{-1}$ ) <sup>a</sup>			
	$\text{MnO}_4^-$	$\text{Cr}_2\text{O}_7^{2-}$	PLS		PCR	
			$\text{MnO}_4^-$	$\text{Cr}_2\text{O}_7^{2-}$	$\text{MnO}_4^-$	$\text{Cr}_2\text{O}_7^{2-}$
1						
2	0.5	13.0	0.53(106.0)	12.20(93.8)	0.51(102.0)	12.5(96.1)
3	3.0	13.0	3.20(106.6)	13.38(102.9)	3.24(108.0)	13.20(101.5)
4	4.0	8.0	3.79(94.7)	7.56(94.5)	4.1(102.5)	8.20(102.5)
5	4.0	12.0	4.22(105.5)	11.94(99.5)	3.80(95.0)	12.40(103.3)
6	5.0	11.0	4.80(96.0)	11.60(105.4)	5.30(106.6)	11.20(101.8)
7	5.0	14.0	5.25(105.0)	13.73(98.1)	5.20(104.0)	14.10(100.7)
8	5.0	17.0	4.76(95.2)	16.45(96.7)	4.95(99.0)	16.70(98.2)
9	7.0	14.0	7.29(104.1)	14.7(100.5)	6.90(98.5)	14.1(100.7)
	10.0	14.0	9.78(97.8)	14.58(104.1)	10.13(101.3)	13.99(99.9)
Mean Recovery			101.7	101.1	102.0	100.5
RMSEP (%)			4.80	3.30	3.17	2.04
RSEP (%)			5.30	3.30	3.17	2.04
R <sup>2</sup>			0.9980	0.9998	0.9995	0.9990

<sup>a</sup>Recovery percent is in parenthesis. Predicted values and recovery percents are averages of three replicates.

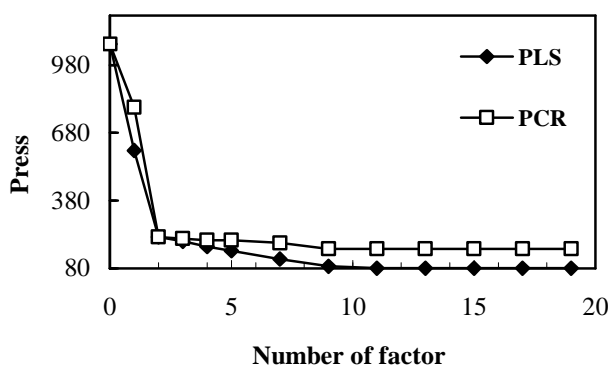


**Fig. 5.** Plot of PRESS against the numbers of factors PLS (◆) and PCR (■). Conditions as in Fig. 1.

squares of correlation coefficient ( $R^2$ ), which are indicatives of the quality fit of all the data to a straight line, were used as follows [38,40]:

$$RMSEP = \left( \sum_{i=1}^N (\hat{C}_i - C_i)^2 / n \right)^{1/2} \quad (16)$$

$$RSEP(\%) = \left( \sum_{i=1}^N (\hat{C}_i - C_i)^2 / \sum_{i=1}^N (C_i)^2 \right)^{1/2} \times 100 \quad (17)$$

$$R^2 = \sum_{i=1}^N (\hat{C}_i - C')^2 / \sum_{j=1}^N (C_j - C')^2 \quad (18)$$

where  $\hat{C}_i$  represents the estimated concentration,  $C_i$  and  $n$  are the actual analyte concentration and the number of samples, respectively.

Table 6 shows the values of RSEP, RMSEP and  $R^2$  for each component using PLS and PCR. It is shown that the obtained values, for the statistical parameters, are almost the same for both PLS and PCR methods.

### Interference Study

The study of interference ions was carried out by a standard mixture solution containing  $10 \mu\text{g ml}^{-1}$  of both  $\text{MnO}_4^-$  and  $\text{Cr}_2\text{O}_7^{2-}$  and a certain amount of foreign ions. The following excesses of ions did not interfere (*i.e.*, caused a relative error of less than 5%): more than a 1000-fold (largest amount tested) amount of  $\text{Na}^+$ ,  $\text{K}^+$ ,  $\text{Zn}^{2+}$ ,  $\text{Cu}^{2+}$ ,  $\text{Cd}^{2+}$ ,  $\text{Mg}^{2+}$ ,  $\text{Be}^{2+}$ ,  $\text{Bi}^{3+}$ ,  $\text{As}^{3+}$ ,  $\text{Cl}^-$ ,  $\text{NO}_3^-$ ,  $\text{BO}_3^{3-}$ ,  $\text{C}_2\text{O}_4^{2-}$ ,  $\text{CH}_3\text{COO}^-$ ; a 100-

fold amount of  $\text{Mn}^{2+}$ ,  $\text{Ni}^{2+}$ ,  $\text{Co}^{2+}$ ,  $\text{pb}^{2+}$ ,  $\text{Cr}^{3+}$ ,  $\text{Ca}^{2+}$ ; a 10-fold amount of  $\text{SO}_4^{2-}$ ,  $\text{PO}_4^{3-}$ ,  $\text{Hg}^{2+}$  and a 1-fold amount of  $\text{Al}^{3+}$ ,  $\text{Fe}^{3+}$ ,  $\text{Zr}^{4+}$ ,  $\text{Ti}^{4+}$ ,  $\text{Mo}^{6+}$ ,  $\Gamma$ .

### Application

To evaluate the analytical applicability of the proposed methods (PCR, PLS and HPSAM), we spiked known amounts of both  $\text{MnO}_4^-$  and  $\text{Cr}_2\text{O}_7^{2-}$  into some water samples. The proposed methods were applied to determine the analytes simultaneously and satisfactory results were obtained (Table 7). The results show that the proposed models could accurately determine the concentration of the oxidants under investigation in real water samples, and there is no significant difference between the results of applying HPSAM, PCR and PLS to their simultaneous determination.

**Table 7.** Simultaneous Determination of  $\text{MnO}_4^-$  and  $\text{Cr}_2\text{O}_7^{2-}$  in Different Water Samples<sup>a</sup> Using HPSAM, PCR and PLS Methods

Sample	Spiked ( $\mu\text{g ml}^{-1}$ )		Recovery (%) <sup>b</sup>					
			HPSAM		PLS		PCR	
	$\text{Cr}_2\text{O}_7^{2-}$	$\text{MnO}_4^-$	$\text{Cr}_2\text{O}_7^{2-}$	$\text{MnO}_4^-$	$\text{Cr}_2\text{O}_7^{2-}$	$\text{MnO}_4^-$	$\text{Cr}_2\text{O}_7^{2-}$	$\text{MnO}_4^-$
1	8	0.5	$98.7 \pm 3.6$	$98.0 \pm 4.0$	$103.7 \pm 4.5$	$106.0 \pm 5.4$	$102.2 \pm 3.4$	$104.0 \pm 3.5$
2	2	2	$104.5 \pm 3.5$	$102.0 \pm 3.0$	$107.5 \pm 4.2$	$106.0 \pm 3.8$	$102.5 \pm 3.3$	$98.6 \pm 3.4$
3	12	5	$102.5 \pm 3.6$	$104.0 \pm 3.5$	$102.4 \pm 3.0$	$100.8 \pm 2.4$	$99.2 \pm 3.0$	$102.2 \pm 4.4$
4	18	8	$101.4 \pm 3.2$	$103.0 \pm 2.5$	$97.6 \pm 3.5$	$103.5 \pm 2.4$	$100.0 \pm 2.5$	$104.5 \pm 5.0$
5	10	1	$104.0 \pm 4.5$	$107.2 \pm 5.5$	$103.0 \pm 3.0$	$106.4 \pm 4.4$	$102.8 \pm 3.5$	$106.0 \pm 4.0$
6	5	4	$99.6 \pm 3.3$	$104.0 \pm 4.6$	$102.0 \pm 3.5$	$94.5 \pm 5.2$	$104.4 \pm 4.0$	$105.4 \pm 4.4$
7	0.2	8	$94.5 \pm 3.6$	$103.0 \pm 3.4$	$98.4 \pm 3.0$	$101.5 \pm 2.7$	$100.2 \pm 3.6$	$103.5 \pm 4.5$
8	15	0.4	$105.0 \pm 4.2$	$100.5 \pm 4.0$	$104.0 \pm 3.8$	$97.8 \pm 3.0$	$104.5 \pm 4.3$	$98.0 \pm 3.9$
9	0.3	5	$100.8 \pm 3.2$	$104.5 \pm 4.0$	$96.7 \pm 3.5$	$103.8 \pm 3.4$	$95.2 \pm 4.0$	$103.5 \pm 5.4$
10	18	0.2	$101.4 \pm 3.6$	$98.6 \pm 2.9$	$97.6 \pm 3.0$	$101.5 \pm 3.4$	$104.0 \pm 4.5$	$103.8 \pm 4.0$

<sup>a</sup>Each sample was analyzed four times. Samples 1, 2, 3 and 4 were drinking water sample, 5, 6, 7 and 8 were river water samples and 9 and 10 were well water samples containing  $\text{MnO}_4^-$  and  $\text{Cr}_2\text{O}_7^{2-}$  mixture. <sup>b</sup>Mean of recovery percent  $\pm$  S.D. (four replicates).

## CONCLUSIONS

This work, as the first application of PCR, PLS and HPSAM to the simultaneous determination of the binary

mixture of  $\text{MnO}_4^-$  and  $\text{Cr}_2\text{O}_7^{2-}$ , shows the ability and excellent performance of ISEs as detectors not only for individual determination of produced or consumed ions, but also in the simultaneous kinetic-potentiometric analysis. This is an impressive result in that a simple bi-variate method such as

HPSAM is shown to be comparable with the powerful multivariate PLS and PCR methods. Although PLS is a full data method, the results clearly show that the HPSAM, as a bi-variate method, ensures almost the same accuracy. However, HPSAM as a standard addition method is more time consuming for analyzing a large number of unknown samples in comparison with PLS and PCR methods. The most important characteristics of this work are as follows: (I) The proposed method is quite suitable for the simultaneous determination of  $\text{MnO}_4^-$  and  $\text{Cr}_2\text{O}_7^{2-}$  in complex samples. (II) The proposed method is cheaper than spectrometric or other electrochemical methods. (III) No extraction step was required and hence the use of toxic organic solvents is avoided. In other words, this method is congruent with the principles of green chemistry.

## ACKNOWLEDGEMENTS

The authors would like to express their appreciations to Professor Afsaneh Safavi for her valuable discussion and useful suggestions. This research was supported by the Payame Noor Universities of Ardakan and Sirjan, Iran, for which we express our profound gratitude.

## REFERENCES

- [1] A. Fatiadi, *Synthesis* 2 (1987) 8.
- [2] B.B. Obeng, *Br. J. Clin. Pract.* 22 (1968) 465.
- [3] R.H. Steinberg, *Appl. Spectrochem.* 7 (1953) 163.
- [4] A. Townshend, A.M. Almuaibed, *Microchem. J.* 52 (1995) 77.
- [5] D. Thorburn Burns, N. Chimpalee, M. Harriott, *Anal. Chim. Acta* 225 (1989) 241.
- [6] H. Rajantie, D.E. Williams, *Analyst* 126 (2001) 86.
- [7] M. Bahram, A. Afkhami, *J. Iran. Chem. Soc.* 5 (2008) 352.
- [8] S. Pandey, M.E.R. McHale, A.-S.M. Horton, S.A. Padilla, A.L. Trufant, N.U. De La Sancha, E. Vela, W.E. Acree, *J. Chem. Educ.* 75 (1998) 450.
- [9] F. Bosch-Reig, P. Campino-Falco, A. Sevillano-Cabeza, R. Herraéz-Hemández, C. Molins-Legua, *Anal. Chem.* 63 (1991) 2424.
- [10] S.K. Schreyer, S.R. Mikkelsen, *Sens. Actuat. B* 71 (2000) 147.
- [11] C. Bessant, S. Saini, *J. Electroanal. Chem.* 489 (2000) 76.
- [12] Y. Ni, L. Wang, S. Kokot, *Anal. Chim. Acta* 439 (2001) 159.
- [13] Y. Ni, L. Wang, S. Kokot, *Anal. Chim. Acta* 412 (2000) 185.
- [14] E. Shams, H. Abdollahi, M. Yekhtaz, R. Hajian, *Talanta* 63 (2004) 359.
- [15] E. Shams, H. Abdollahi, R. Hajian, *Electroanalysis* 17 (2005) 1589.
- [16] J. Mortensen, A. Legin, A. Ipatov, A. Rudnitskaya, Y. Vlasov, K. Hjuler, *Anal. Chim. Acta* 403 (2000) 273.
- [17] M. Slama, C. Zaborosch, D. Wienke, F. Spener, *Sens. Actuat. B* 44 (1997) 286.
- [18] B. Hitzmann, A. Ritzka, R. Ulber, T. Scheper, K. Schügerl, *Anal. Chim. Acta* 348 (1997) 135.
- [19] N. García-Villar, J. Saurina, S. Hernández-Cassou, *Anal. Chim. Acta* 477 (2003) 315.
- [20] A.H. Aktas, S. Yasar, *Anal. Chim. Slov.* 51 (2004) 273.
- [21] M. Akhond, J. Tashkhourian, B. Hemmateenejad, *J. Anal. Chem.* 61 (2006) 804.
- [22] Y.-Z. Ye, Y. Luo, *Lab. Robot. Automat.* 10 (1998) 283.
- [23] M.A. Karimi, M. Mazloun Ardakani, H. Abdollahi, F. Banifatemeh, *Anal. Sci.* 55 (2008) 261.
- [24] M.A. Karimi, H. Abdollahi, H. Karami, F. Banifatemeh, *J. Chin. Chem. Soc.* 55 (2008) 129.
- [25] M.A. Karimi, M.H. Mashhadizadeh, M. Mazloun Ardakani, N. Sahraei, *J. Food Drug Anal.* 16 (2008) 39.
- [26] M.A. Karimi, M. Mazloun Ardakani, R. Behjatmanesh Ardakani, M.R. Zand Monfared, *Chem. Anal. (Warsaw)* 54 (2009) 1321.
- [27] M.A. Karimi, M.H. Mashhadizadeh, M. Mazloun Ardakani, N. Sahraei, *J. AOAC Int.* 93 (2010) 327.
- [28] E. Athanasiou-Malaki, M.A. Koupparis, T.P. Hadjiioannou, *Anal. Chem.* 61 (1989) 1358.
- [29] Z.-H. Mo, L.-H. Nie, S.-Z. Yao, *Anal. Chim. Acta* 246 (1991) 421.
- [30] K. Srinivasan, G.A. Rechnitz, *Anal. Chem.* 40 (1968) 509.
- [31] N. Radic, M. Bralic, *Analyst* 115 (1990) 737.
- [32] P. Campins-Falco, F. Bosch-Reig, R. Herraéz-Hernández, A. Sevillano Cabeza, C. Molins Legua,

Application of H-Point Standard Addition Method and Multivariate Calibration Methods

- Anal. Chem. 63 (1991) 2424.
- [33] A. Afkhami, M. Bahram, A.R. Zarei, *Microchim. Acta* 148 (2004) 317.
- [34] M.A. Karimi, M. Mazloun Ardakani, M.R. Hormozinezhad, R. Behjatmanesh Ardakani, H. Amiryani, *J. Serb. Chem. Soc.* 73 (2008) 233.
- [35] M. Hasani, L. Yaghoubi, H. Abdollahi, *Talanta* 68 (2006) 1528.
- [36] M.A. Karimi, M. Mazloun Ardakani, H. Amiryani, *Asian J. Chem.* 20 (2008) 2105.
- [37] K. Nagaraja, Vipul, M. Rajshree, *Anal. Sci.* 23 (2007) 445.
- [38] M. Otto, W. Wegscheider, *Anal. Chem.* 57 (1985) 63.
- [39] H. Abdollahi, *Anal. Chim. Acta* 422 (2001) 327.
- [40] W. Lindberg, J.A. Persson, S. Wold, *Anal. Chem.* 55 (1983) 643.
- [41] D.M. Haaland, E.V. Thomas, *Anal. Chem.* 60 (1988) 1193.
- [42] J. Ghasemi, M. Vosough, *Spectrosc. Lett.* 35 (2002) 153.
- [43] M. Oue, W. Wegscheider, *Anal. Chem.* 57 (1985) 63.